ANALYSIS OF LOW-COST UAV PHOTOGRAMMETRY SOLUTIONS FOR BEACH MODELLING AND MONITORING USING THE OPENSOURCE QUANTUM GIS

M.A. Eboigbe, D. B. Kidner, M. Thomas, N. Thomas, and H. Aldwairy

University of South Wales, Faculty of Engineering and Computing, UK
(mitchell.eboigbe, david.kidner, malcolm.thomas, nathan.thomas, hamzeh.aldwairy) @southwales.ac.uk

KEY WORDS: Low-Cost, UAV Photogrammetry, LiDAR, Beach Modelling, QGIS, Micro-scale

ABSTRACT:

Coastlines are fundamentally unique features. Their behavioural patterns are predominantly subjects of numerous environmental and engineering studies. With the magnitude of the effects of coastal flooding and erosion, there is a need for accurate techniques for data capture and data processing. With an emphasis on the zero-cost open source GIS software, there is no existing evaluative procedure for demonstrating the analytical capabilities of large-scale UAV-based outputs for microscale analysis for small changes on the beach such as sediment movement, erosion/accretion of individual features. There were four different drone surveys in the study area to determine microscale change over time. A three-stage analysis procedure helps in determining the overview of the coastline and highlights the region(s) of optimum change requiring further spatial analysis with micro-scale change detection. Results obtained show the analytical capabilities of large-scale UAV-based outputs for relatively small but detailed analysis using the open-source QGIS. Results obtained show that spatial analyses of the zoomed areas at different viewpoints and scales improve the confidence level of the hillshading and contour of that particular section on the coastline. The UAV photogrammetry and the three-stage analysis procedure can detect a 1cm change on the beach using the free and open-source QGIS software. It shows the profile modelling of the coastal inundations for both pre and post-flooding events at sub-centimetre intervals can be obtained from QGIS modelling, data computation, analysis, and visualization.

1. INTRODUCTION

Beach Modelling and Monitoring are crucial and inevitable (Eboigbe, 2021; Anandabaskaran and Vijayakumar, 2017) and require immediate, reliable, and cost-effective monitoring techniques (Ahmed et al, 2018). Ocean currents result in regular upwelling and downwelling, thereby resulting in frequent coastal flooding and erosion (Eboigbe, 2021; Samanta and Paul, 2016; Ringim et al, 2016; Bio et al, 2015; Chaaban et al, 2012). Shoreline management plans for the South Wales coastline in the UK are typically challenged by the availability of funds for both data capture and data analysis. Apart from the high cost of data accurate data, such as LiDAR, aerial images, and other high and very-high-resolution images (Eboigbe, 2021; Banks et al, 2017; Casella et al, 2014 and Braga et al, 2013), there is also the challenge with acquiring high-cost proprietary software for data processing and analysing (Awange and Kiema, 2018). Regular beach monitoring should include adaptable methodologies for data capture and analysis in terms of frequency and cost (Eboigbe and Kidner, 2020). A long and short-term beach monitoring infrastructure is possible on the availability of regular coastal processes and evolutions (Chang et al, 2018 and Turner et al, 2016).

The beach or shore stretches from the low-tide shoreline to the coastline and includes the foreshore and the backshore (Eboigbe, 2021; Scarelli et al, 2017 and Longhitano, 2015). The beach consists of silt, sand, pebbles, shells, gravel, rocks, and cobbles (Kwarteng et al, 2016). Periodic changes in the low tide and high tide shorelines will help understand the sea wave pattern for resource planning and emergency (Caudle et al, 2019; Rouse et al, 2019; Scarelli et al, 2017; Robinet et al, 2016). The movement of sediment and deposits on the berm and dunes are key factors in understanding several geomorphological processes (Eboigbe, 2021; Naylor et al, 2017; Goncalves and Henriques, 2015). Research by Eboigbe (2021) shows that the tidal wave will result in sediments and/or wash-over (Mulhern et al, 2017). An effective Coastal zone management infrastructure will include therefore the spatial relationship and variability between the nearshore, the shore, and the coast (Joevivek et al, 2018 and Papakonstantinou et al, 2016). Beach transects are periodically represented relative to distances from assigned tidal heights at very accurate and precise x. y, z coordinates (Casella et al, 2016; Theuerkauf and Rodriguez, 2012).

The cartographic and analytical capabilities of the QGIS which includes the beach information infrastructure is well explained in Lemenkova (2020), Eboigbe (2017) and Eboigbe (2021). When compared with the proprietary ArcGIS, the QGIS has the fuctionalities for advanced geospatial analysis and modelling of the beach (Casella et al, 2016). This study, therefore, demonstrates the use of low-cost and large-scale (localised) methodologies for analysing the coastline using a three tier stage analysis. The aim is to detect a change to up to 1cm on a large-fine scale from low-cost UAV photogrammetry and the QGIS for spatial analysis.

2. STUDY AREA

Penarth lies within the Vale of Glamorgan. It is approximately 6.4 kilometres from the Cardiff city centre. It is bounded by the Severn Estuary on the north shore and the Cardiff Bay at the far south. Penarth has the second largest coastal global tidal range and is predominately characterized by frequent coastal flooding and erosion (Eboigbe, 2021; Eboigbe and Kidner, 2020).

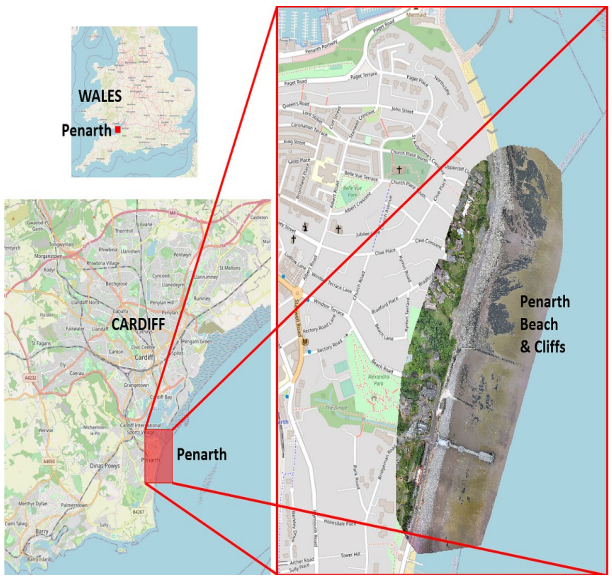

Figure 1 - Case Study Area of Penarth Beach in South Wales, UK.

The sea level rise at the Penarth impacts greatly to changes along the coast and causes damage to the sea defences. Regular flooding along the Penarth coast causes movements on small pebbles, debris, increase/decrease on sandy materials, and even shifts on large, interlocked boulders (figure below)

Figure 2 – Changes on the Penarth Beach Regularly Displaces the Beach Materials

3. METHODOLOGY

This research focuses on the suitability for survey-grade data capture (e.g. centimetre or sub-centimetre accuracy) to be able to model and analyse small changes in coastal environments (e.g. beach volumetric change) (Eboigbe, 2021; Eboigbe and Kidner, 2020). The mapping of the Penarth coastline stretches from the south end of the pier towards the northern side capturing the cliff embankments (see Figure 2). For each of the surveys, the average stretch of the coastline surveyed is an average of 80 acres. Four surveys one in 2015 and 2016 and two in 2020 help to accurately determine the rate of accretion and erosion on the stretch of the coastline being monitored.

3.1 A Three (3) Stage Analyses Procedure

An improvement to existing monitoring techniques is the establishment of a three-stage monitoring technique.

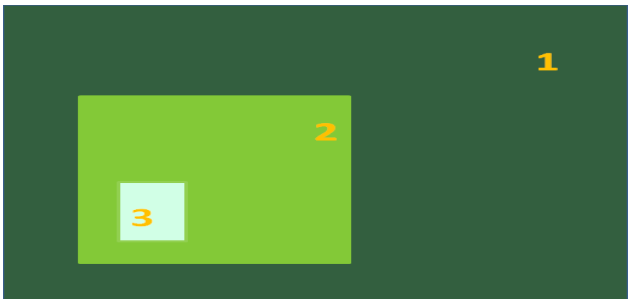

Figure 3 – The Three_Stage Analysis Procedure

Stage 1 is on a small scale. It gives an overview of the coastline in detail with the help of accurate and high-resolution orthomosaics and digital models. Stage 2 in medium-scale focus on the areas where changes have occurred. Stage 3 is the large scale which can detect change for up to 1 cm.

3.1.1 Small Scale Overview and Digitizing of Aerial Photograph

With thanks to Derek Elliott of the Aerial Photography Unit of the National Assembly of Wales, an archive of historic photography of the Penarth area (figure 4) has been supplied and analysed concerning changes of the shoreline through time (i.e. since WWII) (Eboigbe, 2021). It is evident that coastal processes have had an effect on this shoreline and that erosion has occurred. The photographs have been digitised, and subsequently geo-referenced to Ordnance Survey mapping to be able to represent these datasets in a Geographical Information System (GIS) for comparisons with other aerial surveys. The small-scale (high altitude) nature of many of these images allows for a visual comparison, but not for an accurate qualitative and quantitative analysis.

Figure 4 – Vertical Aerial Photograph of Penarth shoreline (10th June 1960) (with thanks to the National Assembly of Wales).

3.1.2 Medium Scale Overview and Spatial Analysis on UAV Images

The digitized AOI is then surveyed from a fully autonomous UAV flight mission using vertical take-off and landing (Eboigbe, 2021; Papakonstantinou et al, 2016). Photogrammetrically, automatic flight control is essential for radiometrically and geometrically precise orthomosaics (Hernandez-Lopez et al, 2013). It also helps to optimize the flight duration (Chiabrando et al, 2017). Due to the topographical nature of the coastlines, the automatic flight

mission from a pre-planned flight plan is required to achieve a higher degree of overlap between images (Chiabrando et al, 2017; Harwin and Lucieer, 2012). It also helps to overcome influences from the external coastal environment such as wind, humidity, sea spray, and other coastal area conditions that could affect UAV performance (Guisado-Pintado et al, 2019).

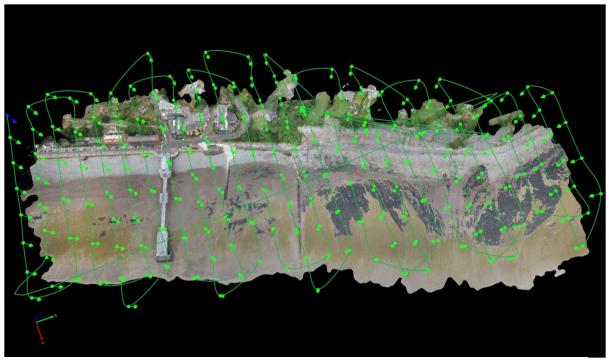

Figure 5 – Trajectory Showing the Flight Path Pattern of the Penarth Survey in 2015 together with the corresponding Orthomosaic.

As all digital images are on the same coordinate systems, spatial manipulations are possible in the open-source Quantum GIS (QGIS). The very high-resolution digital model as derived from the UAVs surveys enhances the computation of volume by determining the areas of cuts and fill as explained in figures 6 and 7 below. Results obtained from this stage then determines the stage 3.

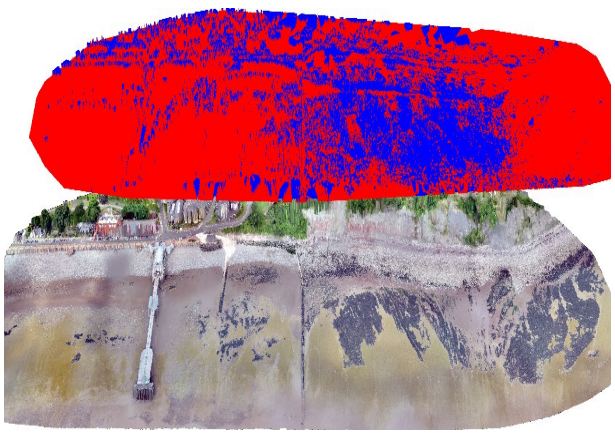

Figure 6 – 2015 DSM with 2016 Orthomosaic. On top is the 2015 DSM showing the areas of cut and fill and the 2016 Orthomosaic below. The red segments on the DSM are the areas of materials loss and the blue segment are the areas of material gains.

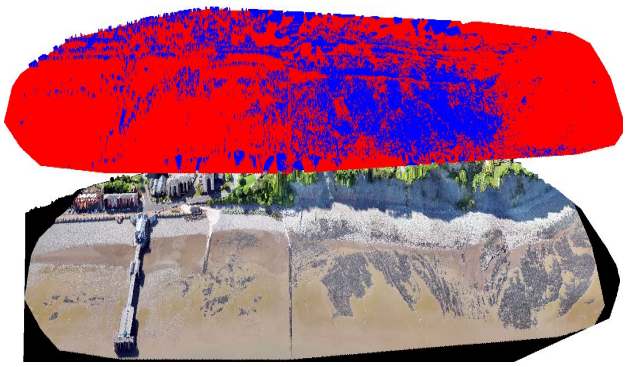

Figure 7 – 2016 DSM with 2015 Orthomosaic. On top is the 2016 DSM showing the areas of cut and fill and the 2015 Orthomosaic below. The red segments on the DSM are the areas of material loss and the blue segment are the areas of material gains.

3.1.3 Large Scale Overview and Further Spatial Analysis on UAV Images

The QGIS extract by mask algorithm extracts the entire cells (including the Z dimension) of the input raster as outlined by the defining mask (Pathan and Agnihotri, 2019; Chamat and Anupriya, 2018). In QGIS, this facility extracts the area of interest in stage 2 of the 3-stage analysis.

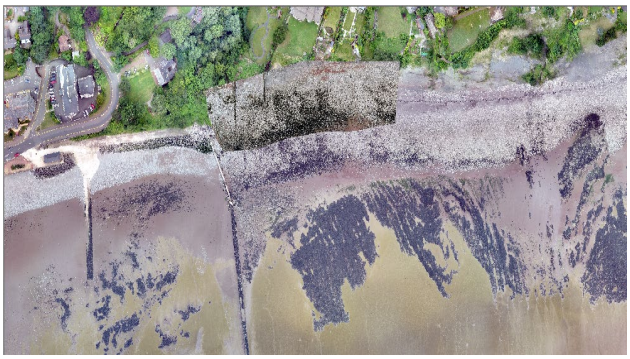

Figure 8 –2015 Penarth Orthomosaic below with Cropped Area on top. The crop area will be further analysed to determine the stage 3.

For stage 3, the digital images will be re-processed for up to 1cm accuracy or by using the extract by polygon tool depending on the accuracy of the initial digital model.

Subsets of the different models are clipped to a common area of the beach for more detailed analysis (Figure 10). Unlike LiDAR, the UAV models generate very high-resolution RGB imagery or point clouds for visual inspection of the surfaces to help understand the differences between surveys.

Figure 9a Penarth UAV 3D Photogrammetric Model 31st July, 2020.

Figure 9b Penarth UAV 3D Photogrammetric Model 2nd August, 2020.

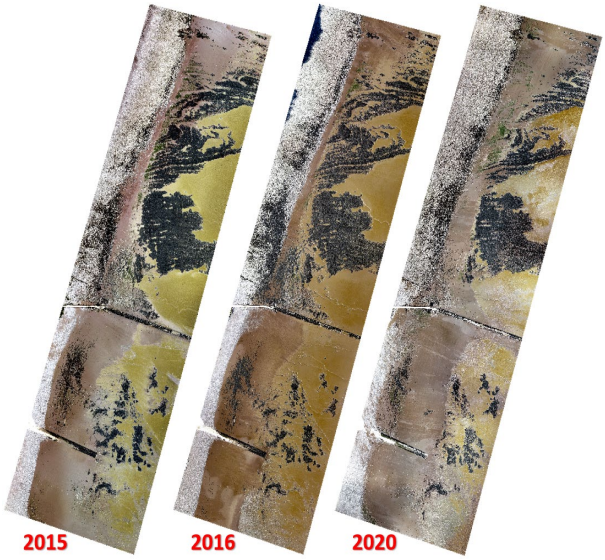

Figure 10 – UAV Orthomosaics of the 2015, 2016 and 2020 Clipped Datasets.

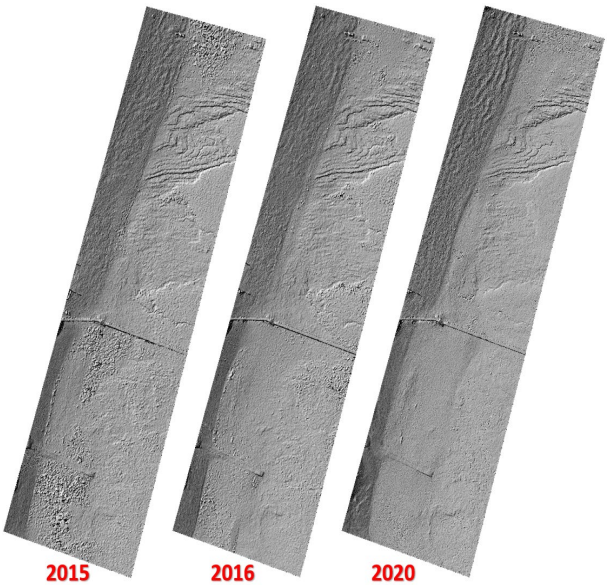

Figure 11 – UAV Hill-Shaded Relief Models of the 2015, 2016 and 2020 Clipped Datasets.

Noteably, the erosion and accretion maps can be generated for the differences between 2020 and 2016 (Figure 11), 2020 and 2015 (Figure 12) and 2016 and 2015 (Figure 13). A better understanding of the results can be accompanied with a visual presentation of the orthomosaics (Eboigbe, 2021).

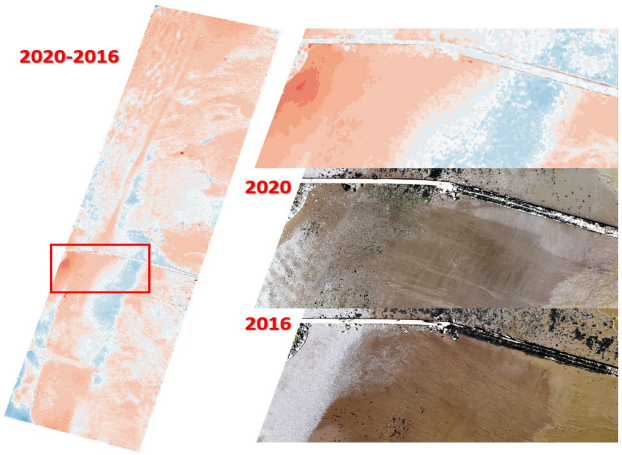

Figure 12 – Erosion/Accretion Map for the UAV Derived Models Between 2020 and 2016.

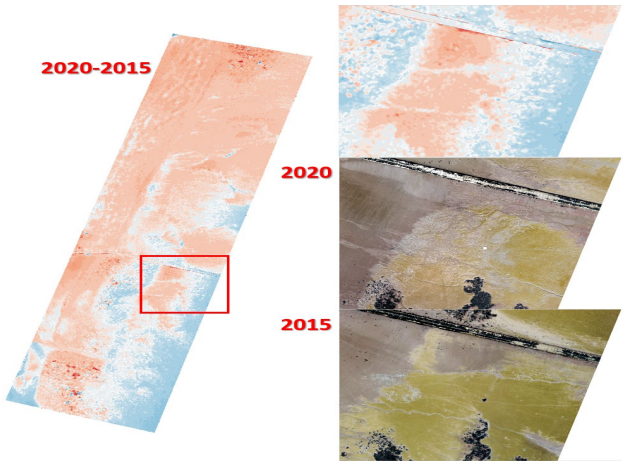

Figure 13 - Erosion & Accretion Map for the UAV Derived Models Between 2020 and 2015

Overall, the map suggests that there is a net loss between the two surveys, but the average loss across the whole of the AOI is about 8cms (as the colour scale is quite small, i.e. any loss is recorded in pink). The Inset maps illustrate a close up view of the area south of one of the outlet casings (cf. groyne) which illustrates intermittent gains and losses in sediment. In general, areas north of this casing have experienced the greatest losses, whilst areas south of this have recorded sediment gains.

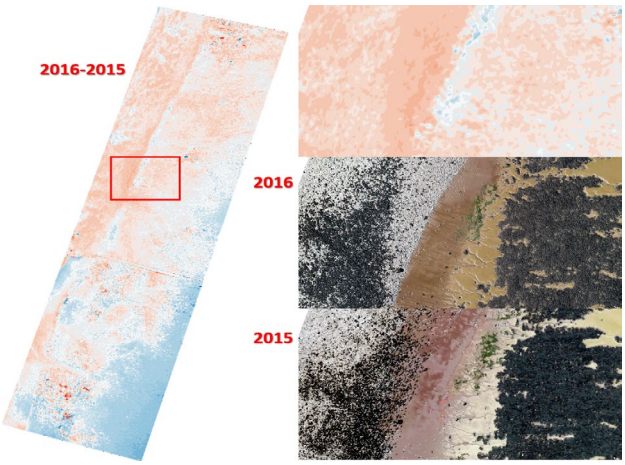

Figure 14 Erosion and Accretion Map for the UAV Derived Models Between 2016 and 2015.

Again, the map demonstrates a net loss of sediment north of the outlet casing and a net loss south of this. The inset map illustrates an area of net loss, but the orthomosaic shows an increase in shingle and stone. However, whilst that may be the case, the underlying sand levels are significantly lower than in 2015. The analysis of Penarth beach using these datasets shows some interesting trends and morphological changes on the foreshore.

4. DISCUSSION OF RESULTS

4.1 Large Scale Analysis of UAV Datasets for Penarth

Consider the two UAV orthomosaics (Fig. 15) captured 48 hours apart. What's changed?

Figure 15 - UAV Orthomosaic for Penarth - Top: 31st July 2020 Bottom: 2nd August 2020.

Figure 15 above illustrates two UAV orthomosaics captured on Friday July 31st 2020 and Sunday August 2nd 2020 (48 hours apart). These solely focus on a zoomed-in section of the datasets of Figure 9a and 9b above respectively. The high tide prior to the first survey was at 10.08m, with subsequent tides at 10.24m, 10.45m, 10.82m, and 10.93m before the second survey. Weather over the 48 hours was very calm, light southerly winds of less than 10mph, and generally warm (maximum of 30 degrees Centigrade on July 31st).

The answer to the above question "what's changed?" is presented below in Figure 16 as an erosion / accretion map. A visual inspection of Figure 15 above might have noticed that the tree trunk close to the cliff face north of the groyne had moved in a southerly direction (and somebody had placed some UAV surveying equipment on the beach!). Otherwise, it is difficult to ascertain much in the way of physical changes. However, Figure 16 suggests that some other changes have occurred. Hopefully, it is noticeable that the movement of the tree trunk is recorded as a red blob in its previous location (i.e. a loss) and a blue blob (i.e. a gain) in its new position.

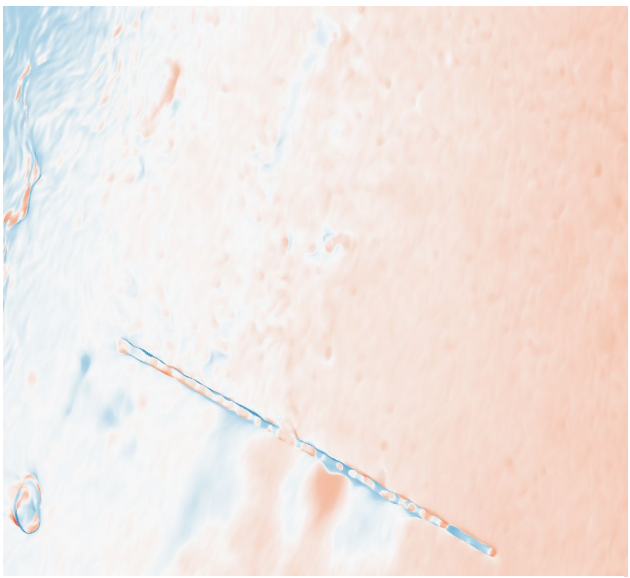

Figure 16 – Erosion / Accretion Map for the two Surveys of Figure 15 (48 hours apart).

The cliff face is represented in blue (a gain), but should not be taken as accurate, since surveying a near vertical structure from a sensor being flown 120 metres above the beach and parallel to it, will only capture a small proportion of points on the cliff surface (Eboigbe 2021. Similarly, the large bush in the bottom left of the maps/images appears both blue and red as some points will be captured differently in the two surveys, i.e. it's not a well-defined object for photogrammetry – nor is any vegetation for that matter. The features close to the cliff face including the tree trunk are illustrated below in Figures 17 and 18.

However, the foreshore should be captured accurately in both surveys, so the predominant pinks and reds suggest that there has been a small loss in sediment over the 48-hour period. The colour scale is defined in centimetres, but nonetheless, the easterly area of this map space suggests that there is a loss in the foreshore of up to 5 cms. Similarly, the area of greatest change in Figure 16 is the red patch just below the groyne. This is worthy of greater examination in Figures 19 and 20. Essentially, the difference map (erosion/accretion) calculation is suggesting that there has been a significant change in sediment in this vicinity, but not immediately clear from the orthomosaics themselves.

On closer inspection, it is worth examining the concrete support (or step) perpendicular to the groyne. In the second figure of 19 the corresponding step on the south side of the groyne is partly exposed (as proven by the red patch in the difference map at this location). Sediment has been moved to expose this step. Of more interest is the larger red blob. From the orthomosaics in Figure 19, it is not instantly clear what has changed or to what extent. By looking at the shaded relief map for the corresponding UAV DSMs (see Figure 20) it is easier to see the

volume of sediment on this part of the foreshore. In the top figure, the sediment appears as a slight mound, which in the second survey has disappeared (or been dispersed).

The amount of sediment loss can be examined further using other traditional analytical tools such as digital contouring and profiling (Figures 21 and 22). Both datasets are contoured in Figure 21, so the differences can be examined more easily than using the erosion/accretion (difference) map. In the location of the larger red blob, there is a three-contour difference (of 5 cms each = 15 cms difference) while northwards of the groyne there is evidence of a longshore drift of 5cms of sediment. These are further visualised as cross-sections either side of the groyne in Figure 22.

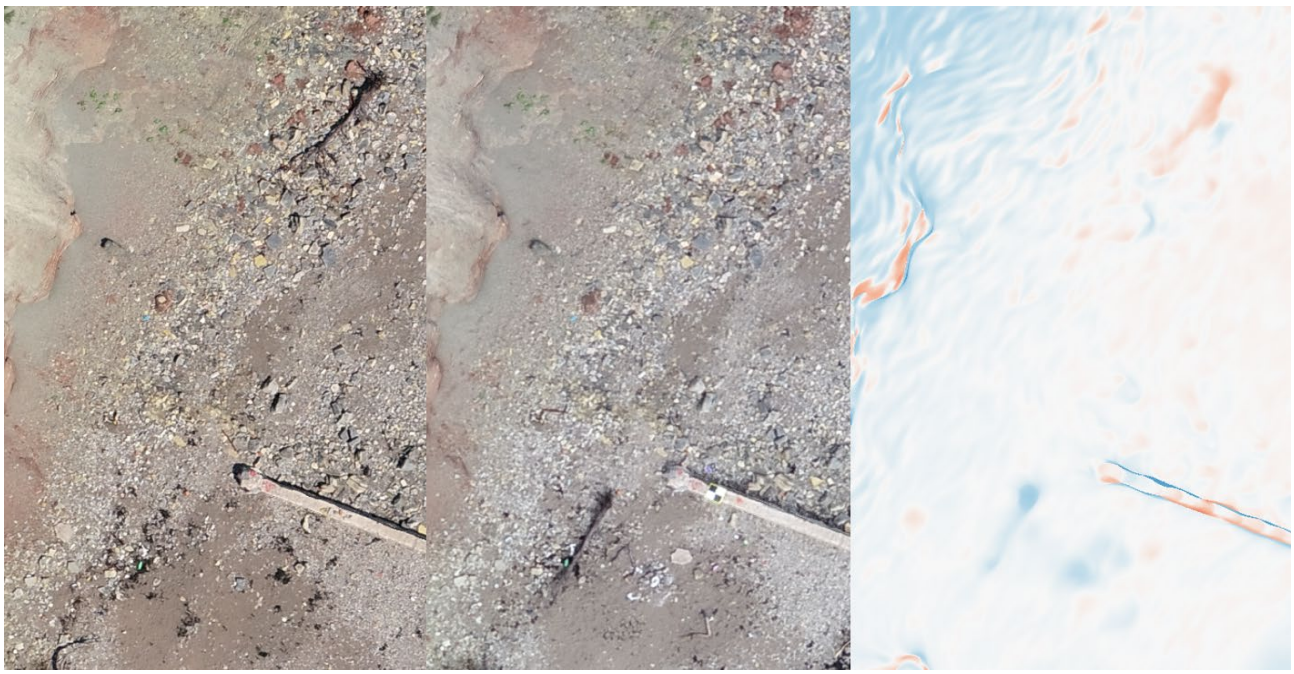

Figure 17 - Zoomed section of the beach near to the cliff face highlighting the movement of the tree trunk and the corresponding erosion/accretion map. (Left: Survey 1; Middle: Survey 2: Right: Difference Map).

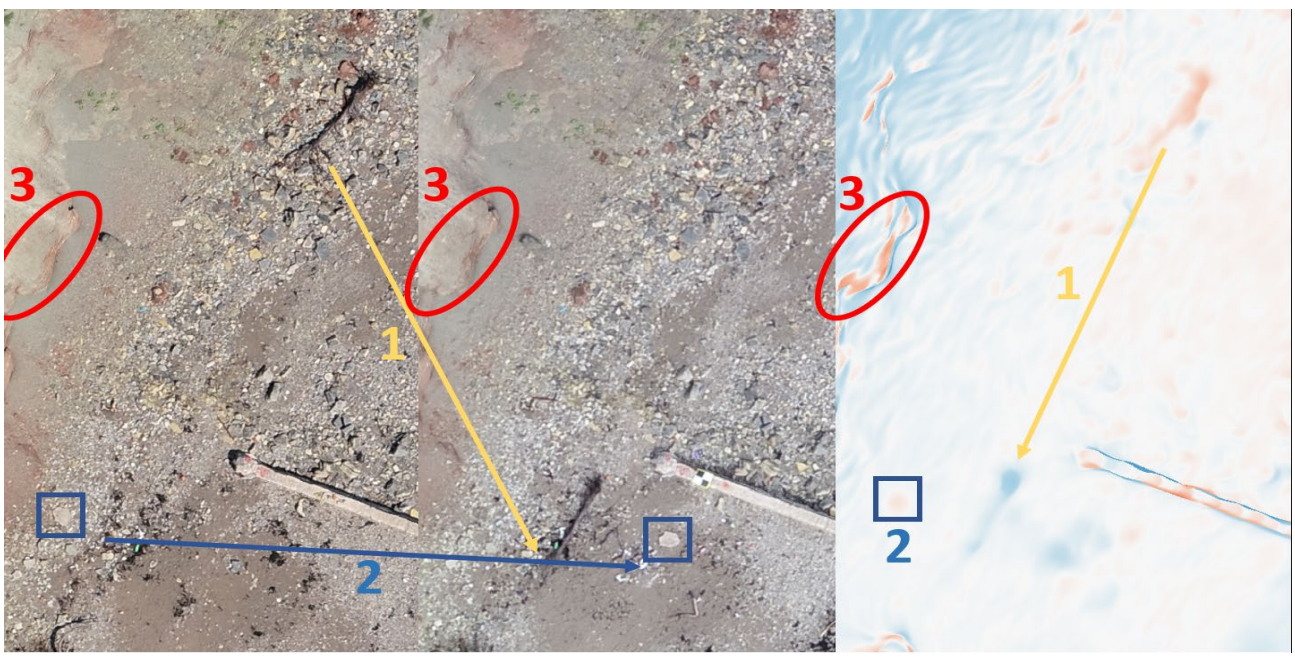

Figure 18 - Zoomed Section of the Beach Near to the Cliff Face Highlighting the Movement of the Tree Trunk (1); the movement of a slab of rock (2) which is identified as a loss (slight pink) in the difference map; and some displacement of the very fine stones/scree at the base of the cliff (3). (Left: Survey 1; Middle: Survey 2: Right: Difference Map).

Figure 19 - Close-up View of the Area around the Groyne. (Survey 1, 2 and Difference Map respectively).

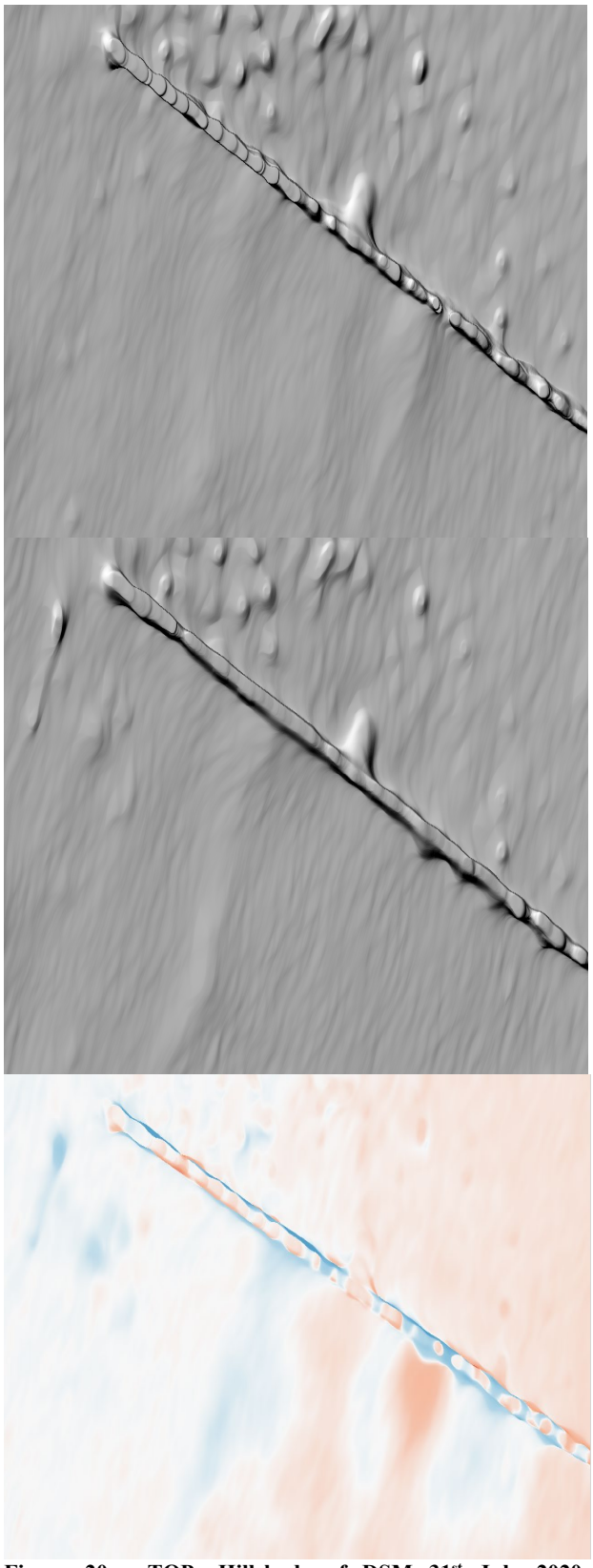

Figure 20 - TOP: Hillshade of DSM 31st July 2020, MIDDLE: Hillshade of DSM 2nd August 2020, BOTTOM: Erosion (Red) / Accretion (Blue) Over the 48-Hour Period.

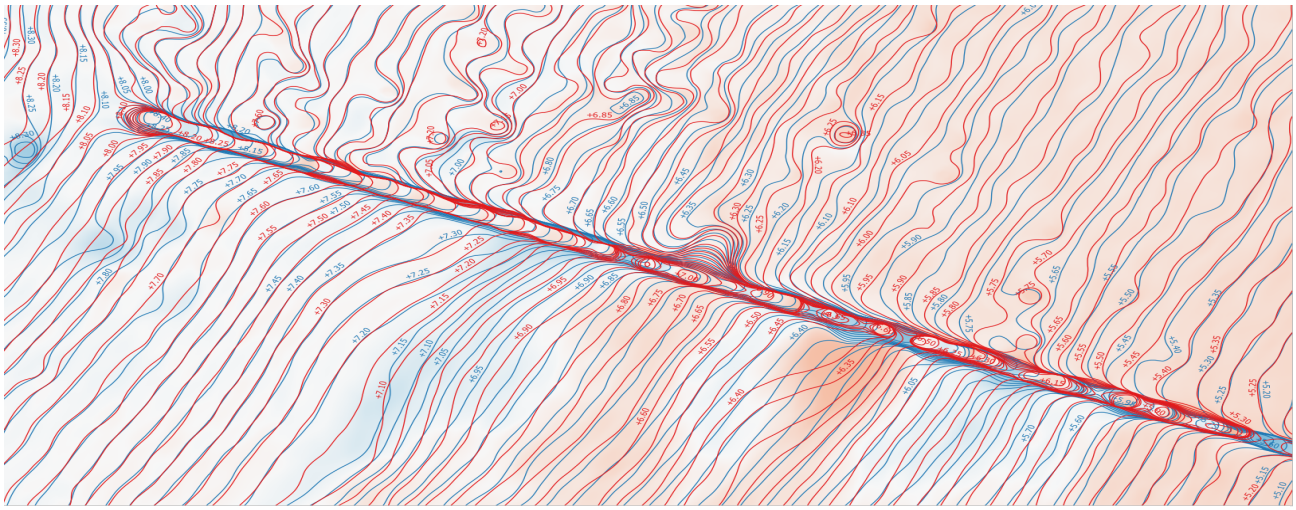

Figure 21 - Erosion (Red Areas) / Accretion (Blue Areas) over the 48-Hour Period between 31/07/2020 and 02/08/2020. The Red Contours denote the first survey and the blue contours denote the second survey (contours are at 5cm intervals). Northeast of the groyne, the pink area denotes a typical sediment loss of 5cms, probably due to longshore drift; while south of the groyne there are bands of erosion and accretion, i.e. the groyne has disrupted the prevailing longshore drift. The area of most erosion (red patch) exhibits a 3-contour interval or 15cms loss of sediment and pebbles.

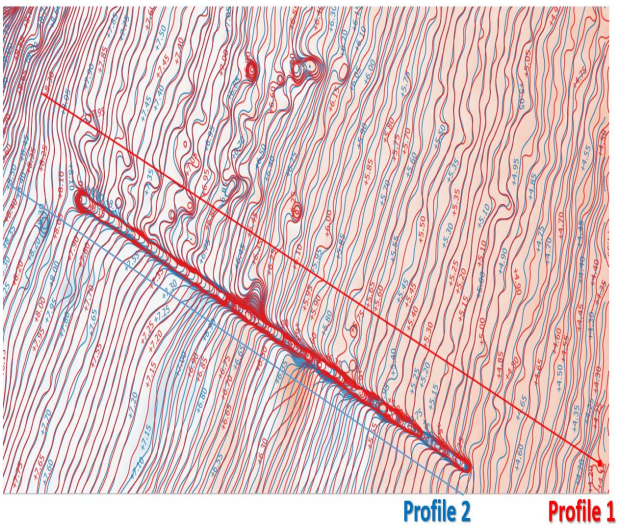

Figure 22a - Location of Two Profile Cross Sections (Profile 1 and Profile 2: North and South of the Groyne).

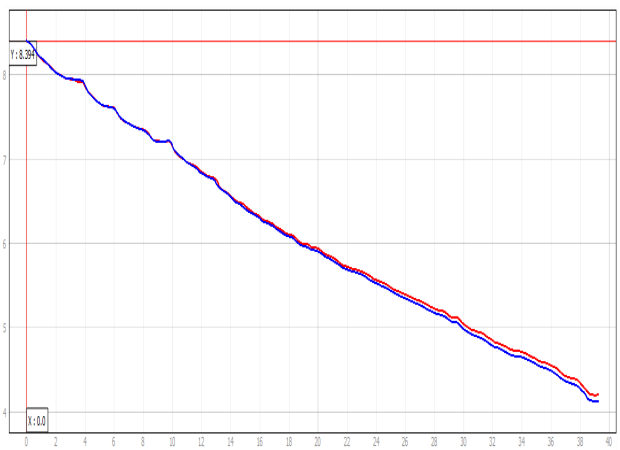

Figure 22b - Profile 1 Cross Section illustrates the red line (1st survey) is approximately 5cms above the blue line (2nd survey 48 hours later) after 20 metres.

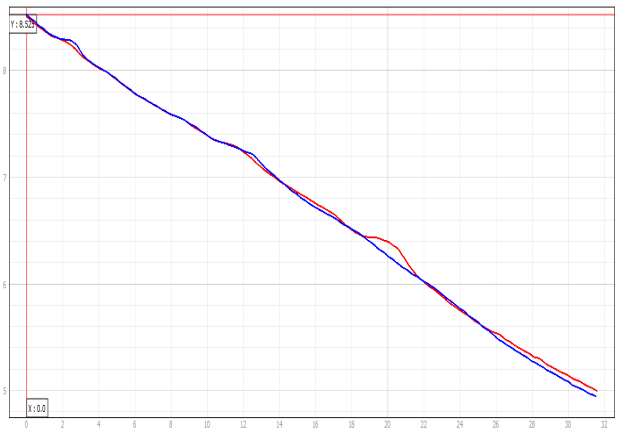

Figure 22c - Profile 2 Cross Section illustrates the intermittent crossing of the red line (1st survey) and blue line (2nd survey 48 hours later) indicating areas of both erosion and accretion. The big difference at 20m indicates a loss in elevation (erosion) between 15 and 20cms.

These analyses show that even though the two surveys were undertaken just 48 hours apart on a very calm weekend of warm, sunny weather with very light winds, the effect of the tides on Penarth beach have had a significant volumetric change of sediment on the beach. This analysis has also demonstrated that UAV photogrammetric models can clearly map, model and identify these changes on the foreshore. All of this modelling was undertaken using free and open-source software.

One other area of further mention is the issue of modelling changes in the cliff face from aerial (vertical) imagery from drones. In Figure 17 and 18 it was suggested that some changes in the cliff face had been identified in the volumetric analysis. Vertical photography will identify the outlier points (or protruding features) of the cliff face, but clearly not the recesses of the cliffs. However, these outliers may have some value in identifying changes to the cliff face, as there will be far fewer points captured in these 3D models, but are clear indicators of change (erosion). Figure 25 explores this further by considering the contours of the cliff face between the two

surveys, rather than just the erosion/accretion map. The original orthomosaics of the two surveys are presented alongside their corresponding contour maps at 5cm intervals. The dense packing of the contours reveals the shape of the cliff surface, in much the same way as the hillshaded maps revealed the sediment displacement on the beach itself. By comparing these contour maps, more definition is given to the shape of the cliff which is not easily discernible from the orthophotos themselves. The difference map supports these areas of change on the cliff surface. This result is an interesting by-product of such a microscale analysis of very high-resolution data.

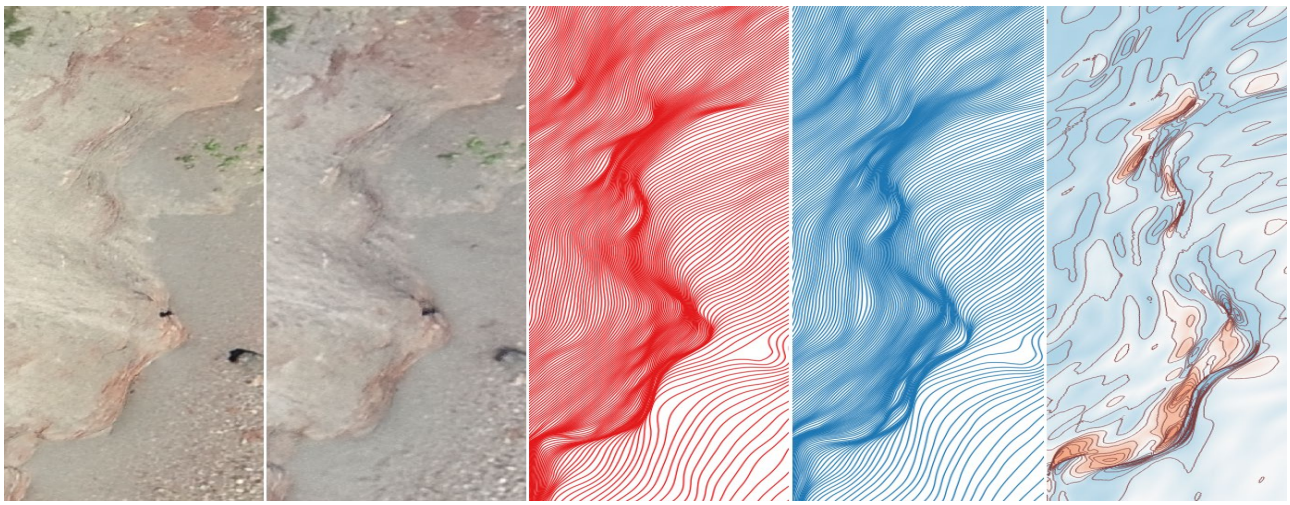

Figure 23 - 3D Digital Orthomosaic for Cliff Analysis. From left to right: 3D Orthomosaic of 31/07/2020; 3D Orthomosaic of 02/08/2010; 5cm Cliff Contours of 31/07/2020; 5cm Cliff Contours of 02/08/2020; Difference Map between 31/07/2020 and 02/08/2020 where the dark pink/orange colours indicate areas of cliff / scree loss which appears to correspond with the difference in shape of the red and blue contours.

5. CONCLUSION

The results obtained in this chapter show the close-range UAV photogrammetry and the three-stage analysis procedure can detect a 1cm change on the beach using the free and open-source QGIS software (Eboigbe, 2021). The cost implication would be less than £350 at the first instance of purchasing the drone and less than £50 (transportation to the site) for other surveys. This procedure has not dismissed the use of the traditional LiDAR or aerial images for beach modelling and monitoring but rather improved on the use of LiDAR, aerial images together with the close-range digital photogrammetry for higher resolution images and accurate spatial and spectral resolution (Eboigbe 2021). The spatial analyses of the zoomed area of Figures 16 -20 at the different viewpoints and scales improve the confidence level of the hillshading and contour of that particular section (Eboigbe, 2021). Spatial analysis of the beach at different scales provides a repetitive beach topography measurement quality (Casella et al, 2020). On its own, it is not possible to obtain the LiDAR datasets at such different scales and with such spectral accuracy. All analyses performed were using the open-source QGIS shows the reliability of the free-to-use GIS software. Figures 10 - 14, 16 – 25 shows that QGIS is excellent in creating accurate 3D models and maps for coastal morphology and visualization. Elevation profiles have been created from the elevation profile plugins. For more interactive and advanced spatial analysis, 3D maps can be created from python based plugins (Eboigbe, 2017). The procedure are enumerated in carrying out the spatial analysis in the QGIS, therefore, becomes a standard for beach monitoring. The contribution to knowledge, therefore, is that technically there is the LiDAR and aerial images at the regional scale, open source QGIS with improved methodology ‘the three-stage analysis’ for accurate spatial analysis and low-cost viability for coastal monitoring

REFERENCES

Ahmed, A., Drake, F., Nawaz, R. and Woulds, C. (2018) ‘Where is the Coast? Monitoring Coastal Land Dynamics in Bangladesh: An Integrated Management Approach Using GIS and Remote Sensing Techniques’, *Ocean and Coastal Management* 151 pp. 10-24. *Science Direct* [Online]. Available at: https://www.sciencedirect.com/science/article/pii/S0964569117306397 (Accessed: 20th November 2018).

Anandabaskaran, V. and Vijayakumar, G. (2017) ‘Monitoring Shoreline Changes of the Puducherry Coast, Souh India: A Review and a Case Study’, *International Journal for Research in Applied Science and Engineering Technology (IJRASET)* 5(XI) pp. 2470-2477. *IJRASET* [Online]. Available at: https://www.ijraset.com/fileserve.php?FID=11658 (Accessed: 01 April 2018).

Awange, J. and Kiema, J. (2018) ‘ Fundamentals of GIS’, in (ed.) *Environmental Geoinformatics. Environmental Science and Engineering*, Springer, Cham. pp 203-212. Springer [Online]. Available at: https://doi.org/10.1007/978-3-030-03017-9_14 (Accessed: 11 March 2022).

Banks, S., Millard, K., Behnamian, A., White, L., Ullmann, T., Charbonneau, F., Chen, Z., Wang, H., Pasher, J. and Duffe, J. (2017) ‘Contributions of Actual and Simulated Satellite SAR Data for Substrate Type Differentiation and Shoreline Mapping in the Canadian Arctic’, *Remote Sensing* 9(12) pp. 2-27. *MDPI* [Online]. Available at: https://www.mdpi.com/2072-4292/9/12/1206 (Accessed: 05 November 2019).

Bio, A., Bastos, L., Granja, H, M., Pinho, J. L. S., Goncalves, J. A., Henriques, R. F, Madeira, S., Magalhaes, A. and Rodrigues, D. (2015) 'Methods for Coastal Monitoring and Erosion Risk Assessment: Two Portugueses Case Studies', *Journal of Integrated Coastal Zone Management* 15(1) pp. 47-63. *Repositorium*[Online]. Available at:https://repositorium.sdum.uminho.pt/handle/1822/43284 (Accessed: 23 October 2018).

Braga, F., Tosi, L., Prati, C. and Alberotanza, L. (2013) 'Shoreline Detection: Capability of COSMO-SkyMed and High-Resolution Multispectral Images', *European Journal of Remote Sensing* 46(1) pp. 837-853. *Taylor and Francis* [Online]. Available at: https://www.tandfonline.com/doi/abs/10.5721/EuJRS20134650 (Accessed: 02 August 2018).

Casella, E., Drechsel, J., Winter, C., Benninghoff, M. and Rovere, A. (2020) 'Accuracy of Sand Beach Topography Surveying by Drones and Photogrammetry', *Geo-Marine Letters* 40 pp. 255-268. *Springer* [Online]. Available at: https://link.springer.com/article/10.1007/s00367-020-00638-8 (Accessed: 11 November 2021).

Casella, E., Rovere, A., Pedroncini, A., Mucerino, L., Casella, M., Cusati, L. A., Vacchi, M., Ferrari, M. and Firpo, M. (2014) 'Study of Wave Runup Using Numerical Models and Low-Altitude Aerial Photogrammetry: A Tool for Coastal Management', *Estuarine, Coastal and Shelf Science* 149(5) pp. 160-167. *ScienceDirect* [Online]. Available at: https://www.sciencedirect.com/science/article/pii/S0272771414002273 (Accessed: 24th October 2018).

Casella, E., Rovere, A., Pedroncini, A., Stark, C. P., Casella, M., Ferrari, M. and Firpo, M. (2016) 'Drones as Tools for Monitoring Beach Topography Changes in the Ligurian Sea (NW Mediterranean)', *Geo-Marine Letters* 36(2) pp. 151-163. *Springer* [Online]. Available at: https://link.springer.com/article/10.1007/s00367-016-0435-9 (Accessed: 03 April 2019).

Caudle, T. L., Paine, J. G., Andrews, J. R. and Saylam, K. (2019) 'Beach, Dune, and Nearshore Analysis of Sourthern Texas Gulf Coast Using Chiroptera LIDAR and Imaging System', *Journal of Coastal Research* 35(2) pp. 251-268. *JCR* [Online]. Available at: https://www.jcronline.org/doi/full/10.2112/JCOASTRES-D-18-00069.1 (Accessed: 04 April 2019).

Chaaban, F., Darwishe, H., Battiau-Queney, Y., Louche, B., Masson, E., El Khattabi, J. and Carlier, E. (2012) 'Using ArcGIS Modelbuider and Aerial Photographs to Measure Coastline Retreat and Advance: North of France', *Journal of Coastal Research* 28(6) pp. 1567-1579. *JCR* [Online]. Available at: https://www.jcronline.org/doi/abs/10.2112/JCOASTRES-D-11-00054.1 (Accessed: 27 March 2018).

Chamat, L. R. and Anupriya (2018) 'Calculation of Cut and Fill of Earthworks with Quantum-GIS', *International Journal for Scientific Research and Development (IJSRD)* 6(3) pp. 2000-2004. *IJSRD* [Online]. Available at: http://ijsrd.com/index.php (Accessed: 03 January 2021).

Chang, Y., Chu, K., Chuang, L. Z. (2018) 'Sustainable Coastal Zone Planning Based on Historical Coastline Changes: A Model from Case Study in Tainan, Taiwan', *Landscape and Urban Planning*174 pp. 24-32. *ScienceDirect* [Online]. Available at: https://www.sciencedirect.com/science/article/pii/S0169204618300689 (Accessed 26 December 2018).

Chiabrando, F., Lingua, A., Maschio, P and Lose, T. (2017) 'The Influence of Flight Planning and Camera Orientation in UAVs Photogrammetry, A Test in the Area of Rocca San Silvestro (LI), Tuscany', *3D Virtual Reconstruction and Visualization of Complex Architectures*, Nafplio, Greece. 1-3 March. *The International Archives of the Photogrammetry, Remote Sensing and Spatial Information Sciences, Volume XLII-2/W3, ISPRS* [Online]. Available at: https://www.int-arch-photogramm-remote-sens-spatial-inf-sci.net/XLII-2-W3/163/2017/isprs-archives-XLII-2-W3-163-2017.pdf (Accessed: 25 November 2019).

Eboigbe, M. A. and Kidner, D. B. (2020) 'Assessment of the Precision of a Smart-Phone Pole Photogrammetry for a Second-Order Cliff Surface Deformation Studies' *ASPRS 2020 Annual Conference Virtual Technical Program,* 22-26 June. *The International Archives of Photogrammetry, Remote Sensing and Spatial Information Sciences*, *XLIV-M-2-2020, 44*, pp.15-24.
ISPRS [Online]. Available at: https://www.int-arch-photogramm-remote-sens-spatial-inf-sci.net/XLIV-M-2-2020/15/2020/ (Accessed 08 November 2021).

Eboigbe, M. A. (2017) 'Exploring the Cartographic and Analytical Functionalities of Quantum GIS: A Comparative Evaluation with MapInfo', *International Journal for Research and Development in Technology* 8(3) pp. 217-225. *Ijrdt* [Online]. Availabale at: https://www.ijrdt.org/ (Accessed: 10 January 2022).

Eboigbe, M. A. (2021) *Low-Cost, Close-Range Digital Photogrammetry for Coastal Cliff Deformation and Beach Monitoring* Ph.D. thesis. University of South Wales [Online]. Available at: https://pure.southwales.ac.uk/en/studentTheses/low-cost-close-range-digital-photogrammetry-for-coastal-cliff-def (Accessed: 15 July 2022).

Goncalves, J. A. and Henriques, R. (2015) 'UAV Photogrammetry for Topographic Monitoring of Coastal Areas', *ISPRS Journal of Photogrammetry and Remote Sensing* 104, pp. 101-111. *ScienceDirect* [Online]. Available at: https://www.sciencedirect.com/science/article/pii/S0924271615000532 (Accessed: 11 November 2016).

Guisado-Pintado, E., Jackson, D. W. T. and Rogers, D. (2019) '3D Mapping Efficacy of a Drone and Terrestrial Laser Scanner over a Temperate Beach-Dune Zone', *Geomorphology* 328(1) pp. 157-172. *ScienceDirect* [Online]. Available at: https://www.sciencedirect.com/science/article/abs/pii/S0169555X1830504X (Accessed: 15 April 2022).

Harwin, S. and Lucieer, A. (2012) 'Assessing the Accuracy of Georeferenced Point Clouds Produced Via Multi-View Stereopsis from Unmanned Aerial Vehicle (UAV) Imagery', *Remote Sensing* 4(6) pp. 1573-1599. *MDPI* [Online]. Available at: http://www.mdpi.com/2072-4292/4/6/1573 (Accessed: 19 October 2016).

Hernandez-Lopez, D., Felipe-Garcia, B., Gonzalez-Aguilera, D. and Arias-Perez, B. (2013) 'An Automatic Approach to UAV Flight Planning and Control for Photogrammetric Applications: A test Case in the Asturias Region (Spain)', *Photogrammetry Engineering and Remote Sensing* 79(1) pp. 87-98. *Ingentaconnec* [Online]. Available at: https://www.ingentaconnect.com/content/asprs/pers/2013/00000079/00000001/art00006?crawler=true&mimetype=application/pdf (Accessed: 06 August 2018).

Joevivek, V., Chandrasekar, N., Saravanan, S., Anandakumar, H., Thanushkodi, K., Suguna, N. and Jaya, J. (2018) 'Spatial and Temporal Correlation Between Beach and Wave Processes: Implications for Bar-Berm Sediment Transition', *Frontiers of Earth Science* 12(2) pp. 349-360. *Springer* [Online]. Available at: https://link.springer.com/article/10.1007/s11707-017-0655-y#citeas (Accessed: 02 April 2019).

Kwarteng, A. Y., Al-Hatrushi, S. M., Illenberger, W. K. and McLachlan, A. (2016) 'Grain Size and Mineralogy of Al Batinah Beach Sediments, Sultanate of Oman', *Arabian Journal of Geosciences* 9(557) pp. 1-18. *Springer* [Online]. Available at: https://link.springer.com/article/10.1007/s12517-016-2583-7#citeas (Accessed: 17 April 2019).

Lemenkova, P. (2020) 'Python Libraries Matplotlib, Seaborn and Pandas for Visualization Geospatial Datasets Generated by QGIS', *Alexandru Ioan Cuza" din Iasi - seria Geografie*, vol. 64(1), pp. 13-32. *SSRN* [Online]. Available at: https://papers.ssrn.com/sol3/papers.cfm?abstract_id=3699706 (Accessed: 11 January 2022).

Longhitano, S. G. (2015) 'Short-Term Assessment of Retreating vs. Advancing Microtidal Beaches Based on the Backshore/Foreshore Length Ratio: Examples from the Basilicata Coasts (Sourthern Italy)', *Open Journal of Marine Science* 5(1) pp. 123-145. *Scientific Research* [Online]. Available at: https://www.scirp.org/journal/PaperInformation.aspx?paperID=53507 (Accessed: 19 January 2019).

Mulhern, J. S., and Johnson, C. L. and Martin, J. M. (2017) 'Is Barrier Island Morphology a Function of Tidal and Wave Regime?', *Marine Geology*387(1) pp. 74-84. *ScienceDirect* [Online]. Available at: https://www.sciencedirect.com/science/article/pii/S002532271630189X (Accessed: 28 March 2019).

Naylor, L. A., Spencer, T., Lane, S. N., Darby, S. E., Magilligan, F. J., Macklin, M. G., and Moller, I. (2017) 'Stormy Geomorphology: Geomorphic Contributors in an Age of Climate Extremes', *Earth Surface Processes and Landforms* 42(1) pp. 166-190. *Wiley Library* [Online]. Available at: https://onlinelibrary.wiley.com/doi/full/10.1002/esp.4062 (Accessed: 28 March 2019).

Papakonstantinuo, A., Topouzelis, K. and Pavlogeorgatos, G. (2016) 'Coastline Zones Identification and 3D Coastal Mapping Using UAV Spatial Data', *ISPRS Int. Journal of Geo-Information* 5(6),75; pp. 1-14. *MDPI* [Online]. Available at: http://www.mdpi.com/2220-9964/5/6/75 (Accessed: 30 March 2018).

Pathan, A. I. and Agnihotri, P. G. (2019) 'A combined Approach for I-D Hydrodynamic Flood Modeling by using Arc-GIS, Hec-Georas, Hec-Ras Interface – A Case Study on Purna River of Navsari City, Gujarat', *International Journal of Recent Technology and Engineering (IJRTE)* 8(1) pp. 1410-1417. *IJRTE* [Online]. Available at: https://www.ijrte.org/ (Accessed: 03 January 2021).

Ringim, A. S., Sulaiman, I. M. and Lyakurwa, J. V. (2016) 'Implementation of Integrated Coastal Zone Management Approach in the Niger Delta, Nigeria: A Review', *International Research Journal of Environmental Sciences and Studies* 1(3) pp. 43-55. *Prudent Journals* [Online]. Available at: https://prudentjournals.com/about-us/ (Accessed: 14 May 2020).

Robinet, A., Castelle, B., Idier, D., Cozannet, G., Deque, M. and Charles, E. (2016) 'Statistical Modeling of Interannual Shoreline Change Driven by North Atlantic Climate Variability Spanning 2000–2014 in the Bay of Biscay', *Geo-Marine Letters* 36 pp. 479-490. *Springer* [Online]. Available at:http://link.springer.com/article/10.1007/s00367-016-0460-8 (Accessed: 11 December 2016).

Rouse, H. L., Bell, R. G., Lundquist, C. J., Blackett, P. E., Hicks, D. M. and King, D. N. (2017) 'Coastal Adaptation to Climatic Change in Aotearoa New Zealand', *New Zealand Journal of Marine and Freshwater Research*51(2) pp. 183-222. *Taylor and Francis* [Online]. Available at: https://www.tandfonline.com/doi/abs/10.1080/00288330.2016.1185736 (Accessed 23 February 2019).

Samanta, S. and Paul, S. (2016) 'Geospatial Analysis of Shoreline and Land Use/Land Cover Changes Through Remote Sensing and GIS Techniques', *Modeling Earth System and Environment* 2(108) pp. 1-8. *Springer Link* [Online]. Available at: https://link.springer.com/article/10.1007/s40808-016-0180-0 (Accessed: 12 December 2016).

Scarelli, F. M., Sistilli, F., Fabbri, S., Cantelli, L., Barboza, E. G. and Gabbianelli, G. (2017) 'Seasonal Dune and Beach Monitoring Using Photogrammetry from UAV Surveys to Apply in the ICZM on the Ravenna Coast', *Remote Sensing Applications: Society and Environment* 7 pp. 27-39. *ScienceDirect* [Online]. Available at: https://www.sciencedirect.com/science/article/pii/S2352938517300666 (Accessed: 10 August 2018).

Theuerkauf, E. J. and Rodriguez, A. B. (2012) 'Impacts of Transect Location and Variation in Along-Beach Morphology on Measuring Volume Change', *Journal of Coastal Research* 28(3) pp. 707-718. *JCR* [Online]. Available at: https://www.jcronline.org/doi/full/10.2112/JCOASTRES-D-11-00112.1 (Accessed: 01 March 2018).

Turner, I. L., Harley, M. D. and Drummond, C. D. (2016) 'UAVs for Coastal Surveying', *Coastal Engineering* 111 pp. 19-24. *ScienceDirect* [Online]. Available at: https://www.sciencedirect.com/science/article/pii/S0378383916300370 (Accessed: 24 November 2016)